

Cracking analysis of plane stress reinforced concrete structures

*Original*

Cracking analysis of plane stress reinforced concrete structures / Busso, Francesco; Anerdi, Costanza; Bertagnoli, Gabriele. - In: IOP CONFERENCE SERIES: MATERIALS SCIENCE AND ENGINEERING. - ISSN 1757-899X. - ELETTRONICO. - 960:(2020), pp. 1-10. (Intervento presentato al convegno 5th World Multidisciplinary Civil Engineering-Architecture-Urban Planning Symposium – WMCAUS 15-19 June 2020, Prague, Czech Republic tenutosi a Prague nel 15-19 June 2020) [10.1088/1757-899X/960/2/022095].

*Availability:*

This version is available at: 11583/2857076 since: 2020-12-12T10:17:25Z

*Publisher:*

IOP Publishing

*Published*

DOI:10.1088/1757-899X/960/2/022095

*Terms of use:*

This article is made available under terms and conditions as specified in the corresponding bibliographic description in the repository

*Publisher copyright*


(Article begins on next page)

PAPER • OPEN ACCESS

## Cracking analysis of plane stress reinforced concrete structures

To cite this article: Francesco Busso *et al* 2020 *IOP Conf. Ser.: Mater. Sci. Eng.* **960** 022095

View the [article online](#) for updates and enhancements.



**EXTENDED ABSTRACT DEADLINE: DECEMBER 18, 2020**

**239th ECS Meeting**  
with the 18th International Meeting on Chemical Sensors (IMCS)

**May 30-June 3, 2021**

**SUBMIT NOW →**

# Cracking analysis of plane stress reinforced concrete structures

**Francesco Busso, Costanza Anerdi, Gabriele Bertagnoli**

DISEG - Politecnico di Torino, Corso Duca degli Abruzzi, 24, Torino, Italy

[gabriele.bertagnoli@polito.it](mailto:gabriele.bertagnoli@polito.it)

**Abstract.** This article presents the numerical analysis' results of reinforced concrete elements subjected to plane stress in early cracking stage. The elements are modelled by a concrete two-dimensional matrix, discrete reinforcement bars and bond-slip elements. The aim of this study is to investigate the behaviour of RC structures before and after the formation of the first cracks to understand the influence on the crack spacing and width of bar orientation with respect to the crack direction, bar spacing and diameter and presence of shear stresses on the crack. Discrete crack non-linear analysis of elements with reinforcement both orthogonal and skew to the crack directions are performed. The interaction between concrete and steel is ensured by a non-linear bond slip law at the interfaces between the two materials. The crack spacing obtained numerically are compared with the ones calculated using different design codes. The analysis of models with different reinforcement geometries allows individuating and discussing the main factors governing two-dimensional plane stress concrete cracking behaviour.

## 1. Introduction

One of the most studied aspects of concrete, and reinforced concrete (RC) structures, is the cracking process that almost always occurs during the service life of the structure. Cracking in RC structures, even if it is almost unavoidable, is not only aesthetically unpleasant but also a possible cause of structural degradation as the opening of a crack deteriorates the layer of concrete cover, increasing the transport speed of oxygen and aggressive agent around steel bars.

Many studies on the prediction of the crack width grounded on experimental data are available in the literature, like those by Gergely and Lutz [1], Oh and Kang [2], Frosch [3] and Gerstle [4]. Crack width is related to the geometry and position of the reinforcing steel, and to the bond between steel bars and concrete, as presented by Goto [5]. More recent research focuses on the factors that influence the crack width itself, like the works of Balázs [6], Borosnyói et al. [7] and Beeby [8] that evidenced how the transverse reinforcement plays a significant role on the crack spacing. Other researchers investigated the effect of imposed strains on crack width and spacing [9-11].

Nevertheless, most of the literature regards the study of one-dimensional elements subjected to pure tension or bending. Only a few pieces of research have focused on two-dimensional RC structures or on the effect of the interaction between shear stresses and normal stresses on the crack formation and opening [12-16].



## 2. State of the art on cracks spacing in one and two-dimensional elements

The evaluation of crack spacing in one-dimensional elements subjected to pure tension can be done following many different National and International Codes presented in Table 1. The meaning of the symbols of each formulation will not be explained here due to lack of space, therefore the reader can refer to the bibliography.

**Table 1.** Cracks spacing in one-dimensional elements subjected to pure tension

Code	Expression
EN 1992-1-1:2004 [17] and Italian D.M.14/01/2008 [18] + Circ. 617/2009 [19]	$s_{r,max} = k_3 c + k_1 k_2 k_4 \frac{\phi}{\rho_{p,eff}}$
ENV 1992-1-1:1991 [20] and ECP 203-2007 [21]	$s_{rm} = 50 + 0.25 k_1 k_2 \frac{\phi}{\rho_r}$
MODEL CODE 1990 [22]	$l_{s,max} = \frac{\phi_s}{3.6 \rho_{s,eff}}$
MODEL CODE 2010 [23]	$l_{s,max} = k c + \frac{1}{4} \frac{f_{ctm}}{\tau_{bms}} \frac{\phi_s}{\rho_{s,eff}}$
Italian D.M. 09/01/1996 [24] + Circ. 252/1996 [25]	$s_{rm} = 2 \left( c + \frac{s}{10} \right) + k_2 k_3 \frac{\phi}{\rho_r}$
CAN-CSA S474-2004 [26] and SN-NS 3473 E [27]	$s_{rm} = 2 \left( c + \frac{s}{10} \right) + k_1 k_2 \frac{d'_{be} h_{ef} b}{A_s}$
JSCE-2007 [28]	$s_{cr} = 1.1 k_1 k_2 k_3 (4 c + 0.7(c_s - \phi))$

Some observations about the equations of Table 1 should be introduced. EN 1992-1-1:2004, D.M.14/01/2008 + Circ. 617/2009 and MODEL CODE 1990 provide formulations to calculate the maximum values of cracks spacing in the “stabilised cracking” phase, therefore the minimum distance at which two near cracks can occur is half of this value. The symbol  $l_{s,max}$  in MODEL CODE 2010 indicates the minimum cracks distance. Therefore, the maximum spacing is double. In D.M.14/01/2008 + Circ. 617/2009 the following link between average and maximum cracks spacing is assumed:

$$s_{r,max} = 1.7 s_{r,mean} \quad (1)$$

and in MODEL CODE 1990:

$$s_{r,mean} = 2/3 s_{r,max} \quad (2)$$

For two-dimensional plane stress elements only EN 1992-1-1:2004, ENV 1992-1-1:1991, MODEL CODE 1990, MODEL CODE 2010 and ECP 203-2007 propose a formulation that combines one-dimensional results with the well-known geometric relation:

$$s_r = \frac{1}{\frac{\cos(\theta)}{s_{r,y}} + \frac{\sin(\theta)}{s_{r,x}}} \quad (3)$$

in which  $s_{r,x}$  and  $s_{r,y}$  are one-dimensional crack spacing distances and  $\theta$  direction of principal stress in concrete.

## 3. Scope of the present work

In the present work, a nonlinear model for plane stress structures is developed to study the crack spacing and crack opening in two-dimensional environment and compare it with code previsions. A generic plane stress structure has been generated using non-linear finite element software taking into account bond-slip interface between reinforcement bars and concrete matrix.

The structure is reported in Figure 1. It is a rectangular ABCD element with  $x_{dim}$  and  $y_{dim}$  edge dimensions. It is associated with a Cartesian  $[x,y]$  reference system that allows identifying the

directions of reinforcement positions through  $\alpha$  and  $\beta$  angles. Reinforcement bars can be positioned at a constant spacing for each direction, called  $s_\alpha$  and  $s_\beta$ . The reinforcement bars layout identifies portions of concrete laying between the bars that will be called “concrete field” and is highlighted in figure 1.

The loads are applied only to the end nodes of the  $\alpha$  and  $\beta$  reinforcements lying on the side AB, imagining that this side is a fully open crack. The stresses in the bars are called, respectively,  $\sigma_\alpha$  and  $\sigma_\beta$  whereas the reinforcement bars cross section  $A_{s,\alpha}$  and  $A_{s,\beta}$ .

When the horizontal resultant force  $R_H$ , acting on the AB side and calculated with eq. (4), is not zero, tangential stress  $\tau_{AB}$  should be acting on the edge AB to restore horizontal equilibrium.

$$R_H = N_\alpha \sigma_\alpha A_{s,\alpha} \sin(\alpha) - N_\beta \sigma_\beta A_{s,\beta} \cos(\beta) \quad (4)$$

where  $N_\alpha$  and  $N_\beta$  are the total number of loaded bars in direction  $\alpha$  and  $\beta$  respectively. The tangential stress  $\tau_{AB}$  is assumed to be uniformly distributed along AB as follows:

$$\tau_{AB} = \frac{R_H}{x_{dim} z_{dim}} \quad (5)$$

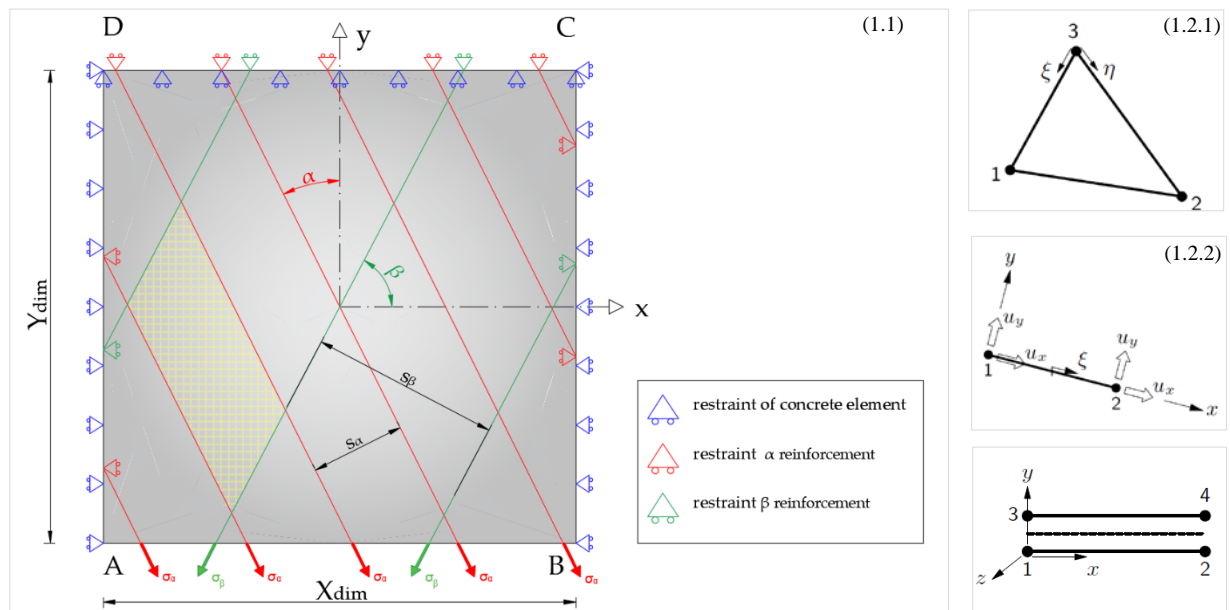


**Figure 1.** (1.1) – RC element general model with dimensions, load stress and restraint layout. (1.2) – Element type used in F.E.M. model: (1.2.1) triangular plane stress, (1.2.2) truss bar, (1.2.3) interface.

The structure presented in figure 1 can be considered a portion of a real element and therefore it is necessary to discuss the boundary conditions. In the present work, the edge CD is placed at a distance from AB that is more than enough to consider the diffusion of stresses from the steel bars to the concrete matrix, completed in the element. Therefore CD edge is considered fully restrained in the y direction. The sides AD and BC represent ideal cuts in a larger structure and are therefore restrained in the x direction.

The concrete mesh is realised with a three-node triangular isoparametric plane stress element (Figure 1.2.1). Reinforcement steel bars are modelled with two-node truss elements with two degrees of freedom per node. Both concrete and steel are considered homogeneous isotropic linear elastic

materials, as the level of stress related to cracking phase justifies this assumption. The interaction between them (bond-slip) is realised using proper interface elements. Bond slip law for these elements is calculated in accordance with specifications of MODEL CODE 2010 for pull out failure and good bond conditions. Young modulus of steel is assumed 200 GPa and concrete class is C25/30.

Different case studies have been performed to approach increasing model complexity as will be presented in the following paragraphs

#### 4. Case study A: one-dimensional tensed element

The one-dimensional problem that has been widely studied and addressed in all codes is the starting point for the calibration of the model. Reinforcing steel bars are parallel to the edge of the concrete matrix so the angles  $\alpha$  and  $\beta$  are null. Main reinforcement, called  $\alpha$ , is placed in the y direction (red in Figure 2) and zero reinforcement in the x direction.

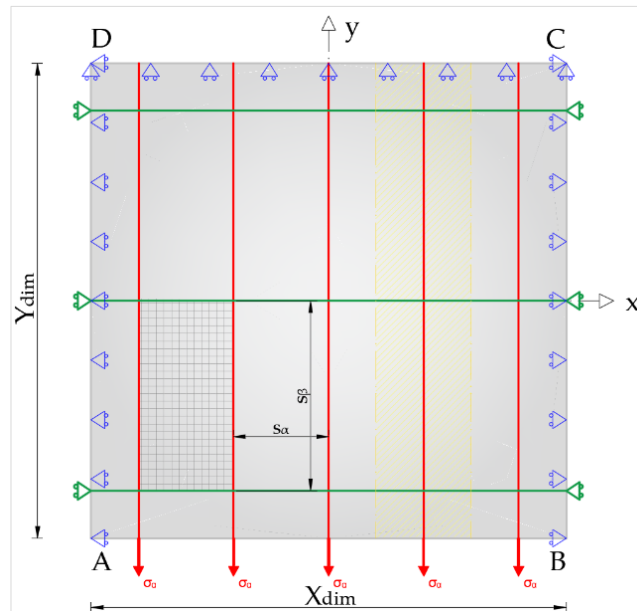


**Figure 2:** Case study A: one-dimensional tensed element

**Table 2.** Subcases A: geometry of one-dimensional tie model, bar diameter, geometrical reinforcement ratio and stress in reinforcement

	$S_\alpha$ [mm]	H [mm]	$\phi_\alpha$ [mm]	$\rho_\alpha$ [%]	$\sigma_\alpha$ [MPa]
A.1	190	100	12	0.60	447
A.2	140	100	12	0.81	333
A.3	90	100	12	1.27	219
A.4	65	100	12	1.77	162
A.5	270	125	16	0.60	446
A.6	200	125	16	0.81	334
A.7	128	125	16	1.27	219
A.8	92	125	16	1.78	161
A.9	350	150	20	0.60	444
A.10	260	150	20	0.81	334
A.11	167	150	20	1.27	219
A.12	120	150	20	1.78	161

The side AB is considered to be the first crack. The stresses  $\sigma_\alpha$ , shown in Table 2, induce crack formation in the tie. It is then possible to determine the distance of the second crack from the AB side,  $y_{cr}$ , as shown in Figure 3. The stresses in the y direction in concrete are varying from zero (on the AB side) to  $f_{ctm}$ . They are not uniform along any line parallel to AB, because of the diffusion from rebars. The red line plotted in figure 3 shows the average stress  $\sigma_{cy}$  in concrete in the function of the abscissa, y. The blue points show the deviation of the stress  $\sigma_{cy}$  from the average at any abscissa y. The first point of the red curve that reaches the tensile strength  $f_{ctm}$  can be assumed as the new cracking point.

The distances  $y_{cr}$  can be considered the minimum crack distances. Their values obtained from the numerical analyses are compared with the relative ones calculated in accordance with the formulations proposed by the codes. The results are summarized in Table 3.

The minimum cracks spacing distances  $l_{tr}$  have been also calculated according to the well-known approach for transmission length calculations derived by a combination of equations (6) and (7).

$$d\sigma_s A_s = A_c f_{ctm} \quad (6)$$

$$\tau_b = d\sigma A_s / (l_{tr} \pi \phi) \quad (7)$$

A graphic representation of the result of Table 3 is presented in Figure 4: graph (a) compares the minimum crack spacing, whereas graph (b) compares the mean crack spacing for the same geometrical configurations. The subcases 1 to 12, listed in Table 3, are arranged along the  $x$  axis in Figure 4. The results, in terms of crack spacing [mm], are plotted along the vertical axis  $y$ .

Numerical results can be directly compared to minimum crack spacing in figure 4(a) and are generally between the results obtained with the formulations proposed by the codes. Crack distance calculated with finite element analysis is generally less sensitive to increasing reinforcement ratio ( $\rho_a$  varying from 0.6% to 1.78% in figure 4(a) whereas the codes provide a higher dependency on this parameter. A good overall agreement between code provisions and numerical simulations can be observed.

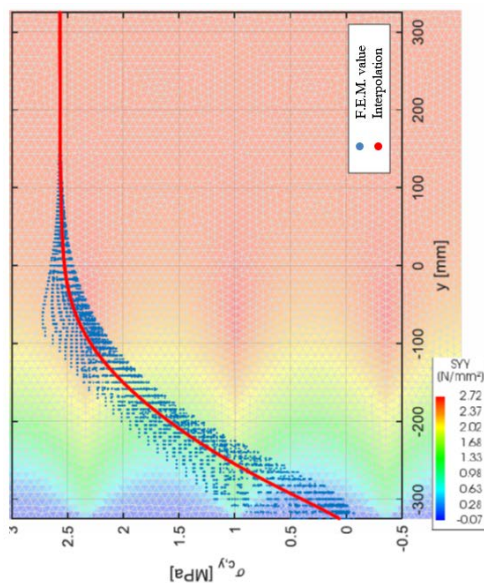


**Table 3.** Minimum crack spacing [mm]. F.E.M results compared with rule value. – Case A

	F.E.M.	EN 1992-1-1:2004	MODEL CODE 2010	MODEL CODE 1990
A.1	327	415	322	278
A.2	268	325	249	205
A.3	232	235	175	131
A.4	214	190	138	94
A.5	430	547	425	371
A.6	340	428	329	274
A.7	280	306	229	175
A.8	256	246	179	125
A.9	530	675	526	461
A.10	425	529	407	342
A.11	326	378	284	219
A.12	295	302	221	156

**Figure 3.** Example case - Concrete  $\sigma_{cy}$  stresses

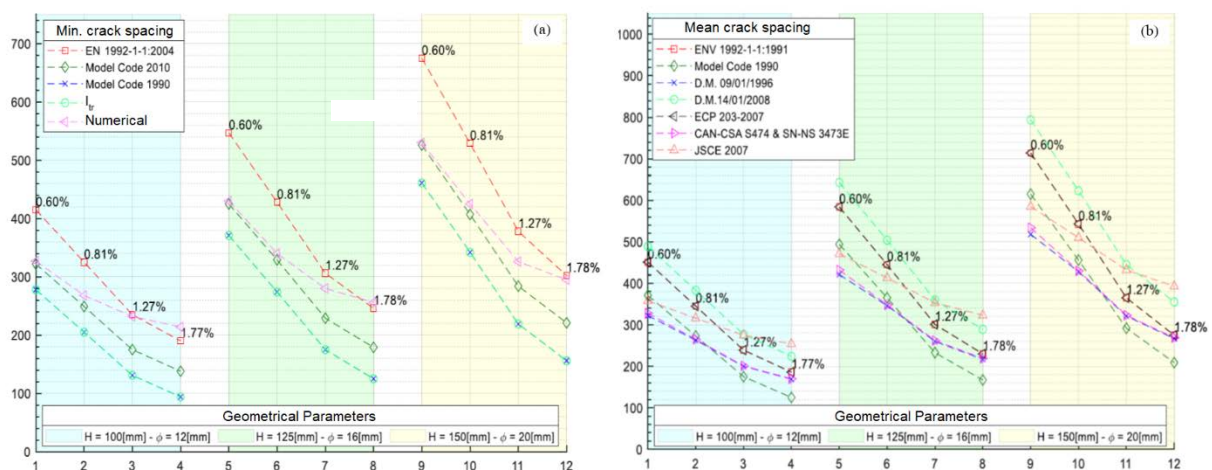


**Figure 4.** (a) – Minimum cracks spacing (b) – Mean cracks spacing



## 5. Case study B

This second case study introduces skew reinforcement with  $45^\circ$  inclination respect to the crack. (angles  $\alpha = \beta = 45^\circ$ ) and the spacing distances  $s_\alpha = s_\beta$  as shown in Figure 5 and described in detail in Table 4. This new structure can still be seen as a simple tie as the stresses in the bars are imposed in order to achieve a uniform tensile stress in the concrete matrix in direction y and almost nil resultant in direction x.

The tensile stresses in reinforcement bars  $\sigma_\alpha$  and  $\sigma_\beta$  are calculated as explained in case A in order to reach stress  $\sigma_{cy}$  equal to the tensile strength  $f_{ctm}$  after diffusion. Only the elements at a certain distance from the sides AD and BC are considered not to take into consideration the perturbations due to the boundary conditions applied on those sides. In fact, stress intensification areas are present along the sides AD and BC (edge effects) caused by the anchoring forces of reinforcing steel bars on the sides. Such anomalies were not present in case study A.

Fourteen cases are studied: the first ten are characterized by uniform reinforcement  $\Phi_\alpha = \Phi_\beta$  and therefore  $\rho_\alpha = \rho_\beta$ , the remaining four with the same reinforcement in  $\alpha$  direction and variable reinforcement in  $\beta$  direction. For the last four sub-cases, it is necessary to determine tangential stresses on the “first crack” AB,  $\tau_{AB}$ , to provide equilibrium in the x direction in accordance with eq. (4) and (5). Crack spacing results from numerical analyses are calculated as shown in Case A. These values should be compared with ones calculated in accordance with eq. (3).

Only EN 1992-1-1:2004, ENV 1992-1-1:1991, Model Code 1990, Model Code 2010 and ECP 203-2007 present equations (3). The results of case study B are shown in Table 5.

In Figure 6 graphic representation of Table 5 data is presented. Along the x axis, the numbers of sub-cases of Table 5 are reported, then along the y axis, the minimum cracks spacing (mm).

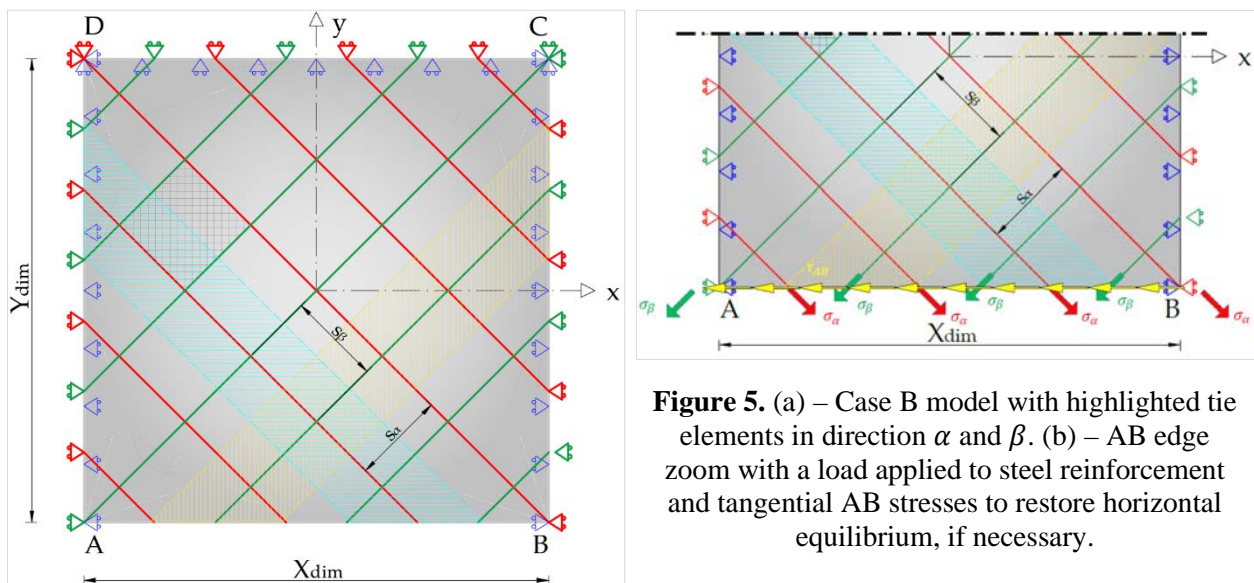


**Figure 5.** (a) – Case B model with highlighted tie elements in direction  $\alpha$  and  $\beta$ . (b) – AB edge zoom with a load applied to steel reinforcement and tangential AB stresses to restore horizontal equilibrium, if necessary.

**Table 4.** Subcases B list with geometry and stress applied to fictitious one-dimensional tie models.

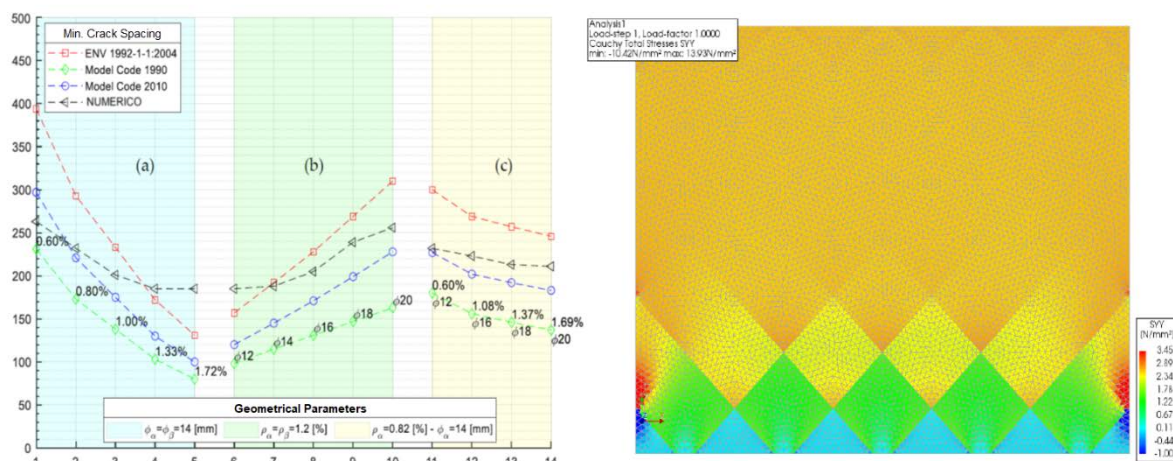
	$B_\beta$ [mm]	$B_\alpha$ [mm]	H [mm]	$\Phi_\alpha$ [mm]	$\Phi_\beta$ [mm]	$\rho_\alpha$ [%]	$\rho_\beta$ [%]	$\sigma_\alpha$ [MPa]	$\sigma_\beta$ [MPa]
B.1	130	130	200	14	14	0.6	0.6	449	449
B.2	130	130	150	14	14	0.8	0.8	340	340
B.3	130	130	120	14	14	1.00	1.00	275	275



B.4	130	130	90	14	14	1.33	1.33	210	210
B.5	130	130	70	14	14	1.72	1.72	166	166
B.6	130	130	73.5	12	12	1.2	1.2	231	231
B.7	130	130	100	14	14	1.2	1.2	231	231
B.8	130	130	130	16	16	1.2	1.2	230	230
B.9	130	130	165	18	18	1.2	1.2	231	231
B.10	130	130	203	20	20	1.2	1.2	230	230
B.11	130	130	145	14	12	0.82	0.6	329	443
B.12	130	130	145	14	16	0.82	1.08	329	255
B.13	130	130	145	14	18	0.82	1.37	329	205
B.14	130	130	145	14	20	0.82	1.69	329	168

**Table 5.** Minimum crack spacing [mm]. F.E.M results compared with rule value – Case B

	One-dimensional model						Two-dimensional eq. (3)			F.E.M.
	EN 1992-1-1:2004		MODEL CODE 1990		MODEL CODE 2010		EN 1992-1-1:2004	MODEL CODE 1990	MODEL CODE 2010	
	$\alpha$	$\beta$	$\alpha$	$\beta$	$\alpha$	$\beta$	-	-	-	
B.1	558	558	326	326	419	419	394	231	297	263
B.2	415	415	244	244	312	312	293	173	221	232
B.3	329	329	195	195	248	248	233	138	175	201
B.4	243	243	146	146	184	184	172	103	130	185
B.5	186	186	113	113	141	141	131	80	100	185
B.6	223	223	139	139	170	170	157	98	120	185
B.7	272	272	162	162	205	205	192	115	145	188
B.8	323	323	185	185	242	242	228	131	171	205
B.9	380	380	208	208	282	282	269	147	199	239
B.10	438	438	231	231	322	322	310	163	228	256
B.11	400	451	236	276	302	343	300	180	227	232
B.12	400	362	236	206	302	271	269	156	202	223
B.13	400	332	236	183	302	246	257	146	192	213
B.14	400	307	236	164	302	226	246	137	183	211

**Figure 6.** Minimum cracks spacing distance and stress distribution of  $\sigma_{c,y}$  in concrete matrix

## 6. Case study C – Moment anomaly

In this chapter is presented a phenomenon that will be called "momentum anomaly". It shows up whenever tangential equilibrium stresses  $\tau_{AB}$  are present on the side AB so it has been noticed in previous sub-cases B.11 to B.14. Tangential stress in these examples had very small intensity so the problem was not evident. In order to detect it,  $\tau_{AB}$  must have appreciable value, so the stresses in reinforcement  $\sigma_\alpha$  and  $\sigma_\beta$  should be significantly different.

The example-model used in this section has the following input data:  $\sigma_\beta = 100$  MPa,  $\sigma_\alpha = 12.5$  MPa,  $N_\alpha = 5$ ,  $N_\beta = 5$ ,  $\phi_\alpha = 16$  mm,  $\phi_\beta = 16$  mm,  $s_\alpha = 150$  mm,  $s_\beta = 150$  mm and the concrete thickness is 100 mm. Steel bars angle  $\alpha$  and  $\beta$  are  $45^\circ$ . Applying equation (5) results that  $\tau_{AB} = 0.59$  MPa is necessary to restore horizontal equilibrium. The concrete displacement field  $u_y$  relative to this case is reported in Figure 7(a).

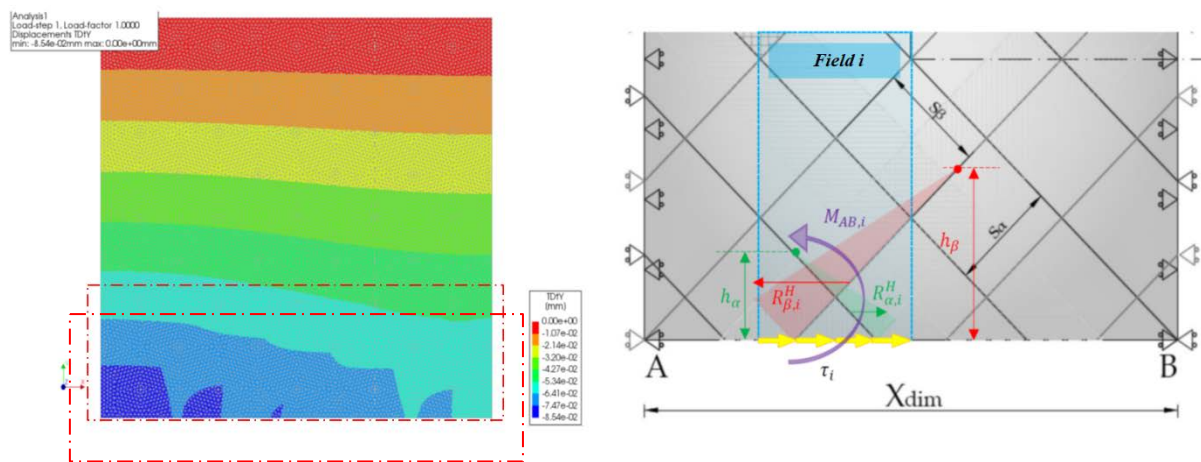


**Figure 7.** (a) – Concrete displacement field  $u_y$ . The dashed line indicates the portion of concrete matrix zoomed in figure (b). (b) – Mechanism of “Momentum anomaly”.

It is clear that the displacement field is not symmetric respect to  $y$  axis. This is the physical representation of the “Momentum anomaly”. The explanation of this missed symmetry can be obtained with the following resisting mechanism. If a simplified triangular bond stress distribution is assumed for bond stresses (between concrete and steel bars), it is possible to define, from F.E.M. results, the forces  $R_{\alpha,i}$  and  $R_{\beta,i}$ . These are the resultant of bond slip stress distribution related to the  $i$ -th concrete field as shown in Figure 7(b). The forces  $R_{\alpha,i}^H$  and  $R_{\beta,i}^H$ , horizontal components of  $R_{\alpha,i}$  and  $R_{\beta,i}$ , equilibrate horizontally the  $\tau_{AB,i}$  stresses, but also generate a moment  $M_{AB,i}$  with respect to the AB side. In fact, assuming triangular bond slip stress distribution,  $R_{\alpha,i}^H$  and  $R_{\beta,i}^H$  are applied to  $1/3$  of the diffusion bond slip stress height  $h_\alpha$  or  $h_\beta$ . The total parasite moment  $M_{AB,i}$  is:

$$M_{AB} = \sum_i M_{AB,i} \quad (8)$$

that is the cause of the non-symmetrical concrete displacement field. To restore local rotation equilibrium, it is possible to apply uniformly distributed tangential stresses to the vertical sides of the concrete element up to mean diffusion height  $l$  starting from point A and from point B, as shown in Figure 8. The value of these stresses is:

$$\tau^* = \frac{M_{AB}}{x_{dim} z_{dim} l} \quad (9)$$

As it can be seen in Figure 8(b), the new concrete displacement field after the correction with  $\tau^*$  stresses results symmetric in the central part where discontinuity anomalies along the vertical edges can be disregarded.

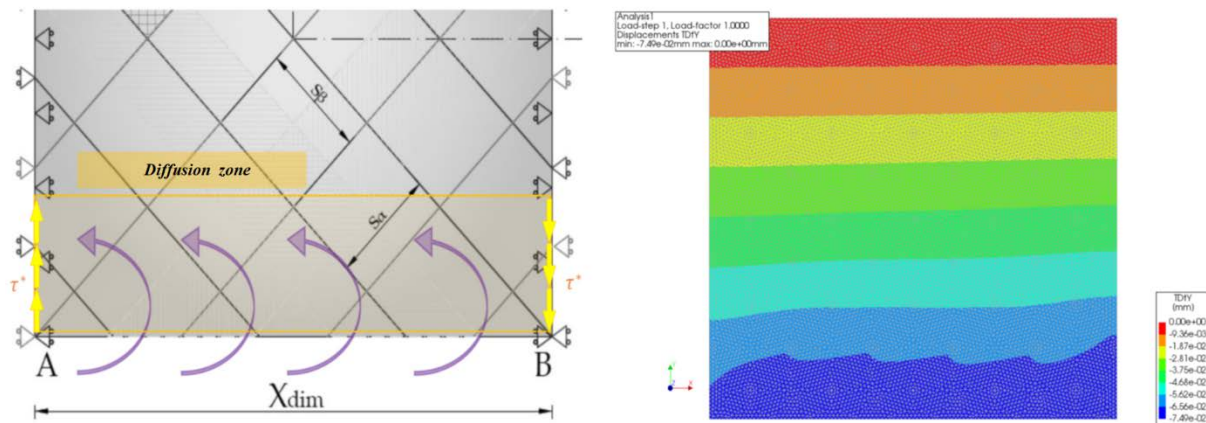


**Figure 8.** (a) – Mechanism to restore local rotational equilibrium avoiding “Momentum Anomaly” – (b) Concrete displacement field  $u_y$  after the application of  $\tau^*$ .

## 7. Conclusions

Observing figure 4 it is clearly evidenced that crack spacing is mainly influenced by the following two parameters: reinforcement steel diameter and geometrical reinforcement ratio. In fact, considering subcases with the same diameter but increasing geometrical reinforcement ratio cracks spacing decreases. Considering the subcases with the same reinforcement ratio but with increasing diameter, the crack spacing also increases. F.E.M. analysis results have a similar trend of respect to code ones. It is interesting to observe that the actual trend of minimum crack spacing F.E.M. results are less sensitive to bar diameter and reinforcement ratio than code results. A similar trend can be recognised in Japanese, Canadian and Norwegian mean crack spacing.

From the observation of Figure 7, the subcases from 1 to 5 present the same bar diameter but an increasing reinforcement ratio, therefore crack spacing decreases. The following subcases from 6 to 10 have the same reinforcing ratio with an increasing diameter: crack spacing increases. The last four cases from 11 to 14 are obtained modifying diameter and reinforcing ratio only in one direction. The effect is a compensation and crack spacing is almost constant.

According to the analyses shown in paragraph 5, it is possible to say that cracking behaviour of two-dimensional RC element seems to be well represented with the model proposed in the codes and derived from the one-dimensional case. The presented two-dimensional model can therefore be validated and highlights some aspects that cannot be seen in the simple one-dimensional tie model, like concrete stress concentration near steel bars or parasite local effects couple that alter local equilibrium for some load conditions. As a conclusion, the proposed F.E.M. approach will be used in the future to study in detail the crack opening in the presence of shear stresses on the crack.

## References

- [1] P. Gergely, L.A. Lutz, “Maxima crack width in RC flexural members, causes mechanism and control of cracking in concrete”, *SP20, American Concrete Institute*, Detroit, pp. 87-117, 1968.
- [2] B.H. Oh, Y.J. Kang, “New formulas for maximum crack width and crack spacing in reinforced concrete flexural members”, *ACI Structural Journal*, Vol. 84, pp. 103-112, 1987.
- [3] R.J. Frosch, “Another look at cracking and crack control in reinforced concrete”, *ACI Structural Journal*, Vol. 96, pp. 437-442, 1999.
- [4] W. Gerstle, A.R. Ingraffea, “Bond in concrete”, Applied Science Publishers, London, 1982.
- [5] Y. Goto, “Cracks formed in concrete around deformed bars in concrete”, *ACI JI*, Vol. 68, No. 2, pp. 244-251, 1971.
- [6] G. Balázs, “Cracking analysis based on slip and bond stresses”, *ACI Materials Journal*, vol. 90, pp.

- 340-348, 1993.
- [7] A. Borosnyói, G.L. Balázs, “Models for flexural cracking in concrete: the state of art”, *Structural Concrete* Vol. 6, No. 2, pp. 53-62, 2005.
  - [8] A.W. Beeby, “The influence of parameter  $\phi/\rho_{\text{eff}}$  on crack widths”, *Structural Concrete*, Vol. 5, No. 2, pp. 71-83, 2004.
  - [9] C. Anerdi, G. Bertagnoli, D. Gino, M. Malavisi, and G. Mancini, “Prediction of Cracking Induced by Indirect Actions in RC Structures”, *World Multidisciplinary Civil Engineering-Architecture-Urban Planning Symposium - WMCAUS 2017*, Prague, 12–16 June 2017. pp. 1-10, 2017.
  - [10] C. Anerdi, G. Bertagnoli, D. Gino, and G. Mancini, “Self restrained cracking of reinforced concrete elements”, *2017 fib Symposium - High Tech Concrete: Where Technology and Engineering Meet*, Maastricht (Ndl), pp. 631-640, 2017.
  - [11] G. Bertagnoli, D. Gino, and G. Mancini, “Effect of endogenous deformations in composite bridges”. *XIII International Conference on Metal Structures (CMS2016)*, Zielona Gora, 15-17 June 2016. pp. 287-298, 2016.
  - [12] P.G. Gambarova, “Sulla trasmissione del taglio in elementi bidimensionali piani di c.a.”, *Atti delle Giornate AICAP* 1983.
  - [13] S.B. Bhide, M.P. Collins, “Influence of Axial Tension on the Shear Capacity of Reinforced Concrete Members”, *ACI Structural Journal*, vol. 86, pp. 570-581, 1989.
  - [14] P. Marti, and J. Meyboom, “Response of prestressed concrete elements to in-plane shear forces”, *ACI Structural Journal*, Vol. 89, pag 503-514, 1992.
  - [15] F.J. Vecchio, and M.P. Collins, “Response of Reinforced Concrete to In-Plane Shear and Normal Stresses”, Publication N. 82-03, Department of Civil Engineering, University of Toronto, 1982.
  - [16] G. Bertagnoli, V.I. Carbone, L. Giordano, and G. Mancini, “Controllo dell'apertura delle fessure in elementi bidimensionali in c.a.”, *Giornate AICAP 2002*, Bologna, 6-8 June 2002, pp. 53-60, 2002 (in italiano).
  - [17] CEN, Comité Européen de Normalisation, “EN 1992-1-1 - Eurocode 2 - Design of concrete structures – Part 1-1: General rules and rules for buildings”, 2004
  - [18] Italian Ministry of Infrastructures, D.M. 14/01/2008, “Norme tecniche per le costruzioni” (in italiano).
  - [19] Italian Ministry of Infrastructures, Circolare 2 febbraio 2009, n. 617 Istruzioni per l' applicazione delle «Nuove norme tecniche per le costruzioni» di cui al decreto ministeriale 14 gennaio 2008 (in italiano).
  - [20] CEN, Comité Européen de Normalisation, “ENV 1992-1-1 Eurocode 2: Design of concrete structures - Part 1: General rules and rules for buildings”, 1991 .
  - [21] Egyptian Ministry of Building Construction, Research Center for Housing, Building and Physical Planning, “Egyptian Code of Practice: ECP 203-2007, Design and Construction for Reinforced Concrete Structures”, Cairo, Egypt, 2007.
  - [22] CEB-FIP Model Code 1990, Design Code, Thomas Telford, June 1991.
  - [23] fib Model Code for Concrete Structures 2010, Wiley, 2013.
  - [24] Italian Ministry of Public Works, D.M. 09/01/1996, “Norma tecniche per il calcolo, l'esecuzione ed il collaudo delle strutture in cemento armato normale e precompresso e per le strutture metalliche” (in italiano).
  - [25] Italian Ministry of Public Works, Circolare n° 252 AA.GG./S.T.C. del 15/10/1996 Istruzioni per l'applicazione delle "Norme tecniche per il calcolo, l'esecuzione ed il collaudo delle opere in cemento armato normale e precompresso e per le strutture metalliche" di cui al decreto ministeriale 9 gennaio 1996 (in italiano).
  - [26] Canadian Standard Associations. S474-04 Concrete structures, 2004.
  - [27] Norway Standard (SN NS), SN NS 3473.E-2004 - Concrete structures - Design and detailing rules Prosjektering av betongkonstruksjoner - Beregnings- og konstruksjonsregler, 2004.
  - [28] JSCE, Japan Society of Civil Engineers, “Standard specifications for concrete structures – 2007 “Design””, 2010.